Proceedings of the ASME 2022 Conference on Smart Materials,
Adaptive Structures and Intelligent Systems
SMASIS2022
September 12-14, 2022, Dearborn, MI

SMASIS2022-90215

FATIGUE ANALYSIS OF BISTABLE COMPOSITE LAMINATE

Shoab Ahmed Chowdhury, Suyi Li, and Oliver J. Myers
Department of Mechanical Engineering, Clemson University
Clemson, South Carolina 29634

ABSTRACT

Bistable composite laminates have exhibited enormous potential in morphing and energy harvesting followed by a wide range of application in aerospace, power generation and automobile industries. This study presents the fatigue analysis of bistable laminates in terms of stiffness degradation and loss of bistability. Moisture saturation of the specimens are ensured by keeping them in a controlled laboratory environment for an extended period of time. Mass of the specimens have been measured to quantify the moisture saturation. Fatigue tests are performed at 1 Hz frequency, and R = -1 stress ratio which is the ratio of minimum stress to maximum stress. Specimens are tested for 3 million cycles in displacement control. Load-displacement plot from the test is divided into 5 stiffness regions. A piecewise study of each region has demonstrated good agreement with existing analytical model. Stiffness degradation in 4 regions corresponding to 2 stable configurations follows general trend for composites up to the second stage of damage in three stage damage progression model while the remaining region corresponding to unstable configuration is not considered in this analysis. Test results have been reproduced with minor discrepancy at the specified environmental and loading condition, ply configuration, and size of the laminate. Test protocols, results, and damage analysis presented in this study can be utilized to evaluate the fatigue performance of multistable CFRP structures subjected to higher amplitudes and frequencies.

Keywords: Bistable, Fatigue, Stiffness Degradation, Damage Evolution

NOMENCLATURE

D (n)	fatigue damage index
E_0	Elastic modulus at the initial cycle
E(n)	Elastic modulus at the nth cycle
E_f	Elastic modulus at the final failure cycle
n	current number of cycles
N	fatigue failure cycle
x	normalized cycle ratio

1. INTRODUCTION

Unymmetric cross-ply laminates exhibit bistable behavior when subjected to elevated temperature and subsequent cooling during fabrication that enable them to acquire two stable cylindrical shapes in response to a small energy input. These equilibrium shapes result from the large deformation in out-of-plane direction effected by the anisotropic properties of the individual layers and the unsymmetric stacking sequence coupled with environmental factors, primarily change in temperature from the processing temperature [1]. Hyer first developed an analytical model to predict the stable shapes of cured thin unsymmetric laminates [2]. Actuation energy required to snap from one stable geometric configuration to another have been attained employing piezoelectric actuators [3] and shape memory alloy wires [4]. Morphing feature of bistbale laminates which is the ability to change shape according to environmental or operational conditions has been studied in aerospace applications [5], wind turbine blades [6], and automobile structures [7]. They can acquire major changes in shape with a discontinuous and small power supply which has inspired new ways of utilizing the stable geometrical shapes [8–13]. Energy harvesting is another exciting implementation of the bistable systems [14]. In many cases, these applications include cyclic loading conditions that can result in fatigue damage of the bistable laminate, but the research study performed in that area has been insubstantial.

Fatigue damage of anisotropic fibre-reinforced composite laminate is much more complex compared to their isotropic metal counterpart. Damages like fibre fracture, matrix cracking, matrix crazing, fibre buckling, fibre-matrix interface failure, delaminations can occur while they can interact with each other and can have different growth rates [15]. Different parameters such as fibre type, matrix type, type of reinforcement structure

*Address all correspondence to this author: shoabac@clemson.edu

(unidirectional, mat, fabric, braiding), laminate stacking sequence, environmental conditions (mainly temperature and moisture absorption), loading conditions (stress ratio R, cycling frequency), and boundary conditions [15] can affect them. Fatigue life models have been developed by Hashin and Rotem to distinguish a fibre-failure and a matrix-failure mode [16]. Phenomenological models based on residual stiffness [17–23], residual strength [24–28] are presented in numerous studies with well defined characterization of fatigue life for a varying range of test conditions. Progressive damage models have also been established to predict damage growth and model damage accumulation for specific damage types, such as matrix cracks and delaminations [29–33]. According to linear elastic fracture mechanics (LEFM), delamination is characterized by introducing the energy release rate, G, referring to the resistance of the material to delamination [34]. It has been investigated by other researchers as major failure mode [35–38] in an effort to develop damage tolerant structures for predicting fatigue life and establishing appropriate inspection intervals. Fatigue damage progression around fastener holes have been found to be driven by the nucleation of delamination associated with increased damage due to delamination observed towards the faying surface of the laminate and (metal) fixture, and at the hole bore surface [39].

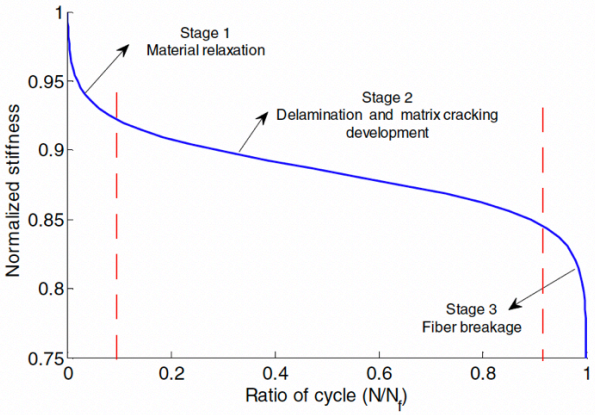

FIGURE 1: GENERAL TREND FOR COMPOSITE STIFFNESS DEGRADATION [40].

Stiffness degradation models proposed by previous studies have successfully captured three stages of damage progression in composite laminates subjected to fatigue loading [40–42] as illustrated in Figure 1. Laminate experiences a sharp drop in stiffness due to matrix cracks. These cracks generate during the preliminary stage which refers to a micro-damage process, and have substantial effects on its residual strength and the life. These cracks grow in multiple numbers and group together during this period and eventually approach to the stable stage. In the second stage, matrix cracks reach the fiber and continue to grow along the fiber-matrix interface. This stage is represented with a larger life span and a lower slope of damage progress. Delamination and matrix cracking drive the gradual decrease in stiffness. The accumulation of these cracks coupled with debonding and delamination during the first two stages induces fiber breakage in the third or final failure stage which is characterized by the rapid drop in stiffness.

Fatigue of composites has been studied extensively while the specific case of bistable laminates has remained mostly unexplored. To the author's knowledge, only one study by Potter has looked into the fatigue response of unsymmetric bistable laminates and reported small reduction in distortion and snapthrough load [43]. Stiffness degradation and damage evolution characteristics due to a cyclic snapthrough and snapback process at out of plane loading is largely unknown. There is also inadequate research done on whether available damage models to capture fatigue response of unidirectional composites are also sufficient for explaining fatigue of bistable laminates. The scope of this paper concentrates on characterizing the stiffness degradation, damage progression and the loss of bistability of the specimen due to out of plane cyclic loading. The test fixture and method developed for the study lays the groundwork for fatigue tests at higher frequencies and a range of boundary conditions. It also enables the protocols for long term application of bistable laminates. Two models from previous studies representing three stage damage progression are evaluated. These models require material dependent parameters to be determined from the test data. A piecewise analysis is implemented to explain the damage evolution that will be elaborated in the subsequent sections. Overall, this study characterizes the fatigue damage of bistable laminates in terms of reduction of stiffness, inspects fatigue effect on bistable performance and proposes updated approach to adopt the existing fatigue damage models for bistable composites that were initially developed for general composites.

Square laminates fabricated from DA 409U/G35-150 with side lengths of 76.2 mm and [0/90] configuration are tested using the Bose Electroforce test system. Test specimens are kept at 55-60% RH until moisture saturation and their masses are measured at a regular interval to ensure that the saturation point has been reached. After moisture saturation, fatigue tests are carried out at a frequency of f = 1 Hz, stress ratio of R = -1 up to 3 million cycles. The specimen is constrained on two corners by means of fasteners while snapthrough and snapback is achieved by applying displacement at the center. Stiffness degradation of the specimen is characterized by dividing the load-displacement plot acquired from test data into 5 stiffness regions. Stiffness degradation analysis over number of cycles is presented for each region. A damage index is defined as a function of stiffness of the specimen to represent the damage progression during the test. An analytical model presented in previous study [44] which was initially developed for fatigue damage prediction in tensile loading condition is implemented for each region individually while determining the model parameters by fitting the test data of the respective region. This piecewise analysis of the damage progression is discussed in terms of the fatigue failure stages of composite material. Finally, a conclusion is drawn on the basis of the test results and the predictive reliability of the model.

2. MATERIAL AND SPECIMEN FABRICATION

Specimens are prepared from DA 409U/G35-150 prepreg which closely resembles the properties of AS4/8552. Properties of both materials are listed in Table 1 for comparison. The roll of the prepreg material is kept in a freezing chamber to store it at a temperature between 0°C and 4°C. Square shaped sections with side lengths of 2 and 3 inches are cut using scissors. To maintain the rigidity of the epoxy resin and to avoid unwanted adhesiveness related issues like fiber distortion, the prepregs are cut while they are still cold. After cutting the sections according to dimensions they are pressed together to form a [0/90] configuration. Then the specimens are cured by following the vacuum bagging method. In this method, a vacuum bagged packet is created in several layers as shown in Fig. 2. An aluminum plate of 0.6m × 0.6m × 4 mm is used as the mold which is covered with a mold release agent. Then a layer of peel ply followed by the uncured samples and another layer of peel ply is placed on the top of the aluminum plate. The subsequent layer is a perforated plastic sheet (10 LYD 3015-PERF-D-Release Ply High Temp 450F- Perforated Film) and after that a sheet of absorbent material (10 LYD 3011-D-Breather Fabric) is placed on top of the perforated sheet. A nozzle is set on the breather fabric and the whole assembly is sealed with double sided tapes. An impermeable vacuum bagging film (10 LYD 3014-D - Stretchlon SL200 Vacuum Bag Film) constitutes the final layer. Finally, the assembled vacuum bag is placed inside the oven and the nozzle is connected to vacuum pump (1 EA. VacuMaster 5 CFM Vacuum Pump) to complete the preparation of vacuum bagged packet.

Before starting the curing process, air is vacuumed out at 35 to 40 psi. Then the curing process starts with preheating the oven to 140°C. The oven is 1.219 m × 1.219 m in dimensions and the internal temperature is controlled by a thermostat. The specimens are cured at this temperature for 1.5 hours and then the oven is turned off to cool the vacuum packet down to room temperature. Once the cooling process is complete the vacuum packet is taken out from the oven. The packet is cut open and the samples are collected. Fig. 2 demonstrates the cured samples of 2×2 and 3×3 inches. Laminates of both sizes have acquired the first stable cylindrical shape which can be snapped to the second stable shape by applying the snapthrough force.

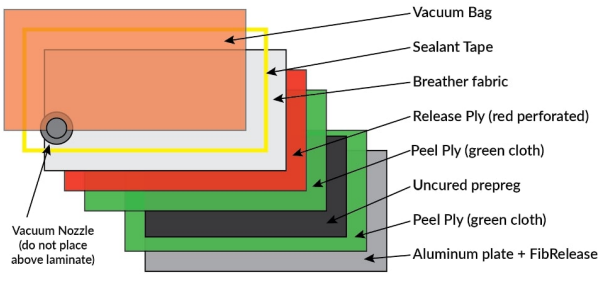

FIGURE 2: PREPARATION OF THE VACUUM BAGGING PACKET

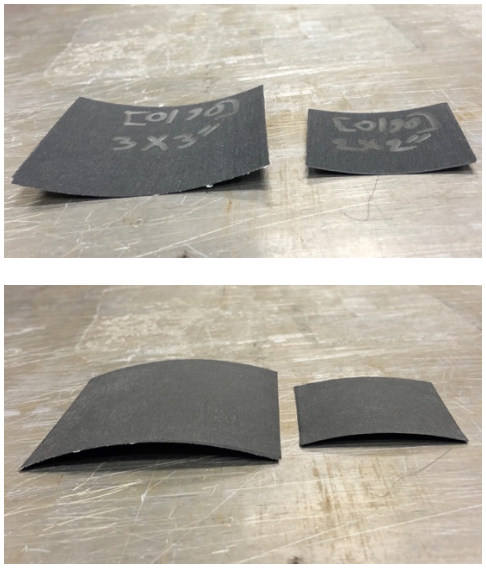

FIGURE 3: TWO STABLE CYLINDRICAL SHAPES OF 2×2 AND 3×3 INCHES SQUARE CROSS-PLY LAMINATE

Material / Property	409U/G35-150	AS4/8552
Tensile Modulus	18.8 Msi (129.6 GPa)	19.6 Msi (135.12 GPa)
Flexural Modulus	17.9 Msi (123.4 GPa)	18.4 Msi (126.85 GPa)

TABLE 1: PROPERTIES OF 409U/G35-150 AND AS4/8552 PREPREGS FOR COMPARISON [45]

3. FATIGUE TEST

3.1 Test Fixture and Conditions

Bistable laminates have been subjected to cyclic load to record and analyze their mechanical response in terms of reduction or loss of bistability and change in stiffness. Specimen is tested in a Bose ElectroForce 3230 system integrated with WinTest 7 software. This system is developed by TA instruments and is capable of doing fatigue test up to 1 billion

cycles. It provides a wide range of parameter control for fatigue tests including frequency up to 200 Hz, load up to 450 N, displacement control over a ±6.5 mm range, and also features a temperature control chamber [46,47].

Fatigue test fixture is constituted by a metal base plate, 3 aluminum bars, screws and fasteners as displayed in Fig. 4. 5-40 fasteners are chosen as they have a small contact surface area with the specimen while allowing a solid mechanical support. This takes care of any excessive or undetermined vibrational motion of the sample during the test which facilitates a smooth load-displacement plot. Supporting bars, plates and the specimen are placed inside the temperature control chamber. This chamber bolsterers the mountings, and also serves as a protective feature for the test fixture from debris created while other activities like fabrication and drilling is done in the laboratory. It can also be used as a constant temperature and moisture control chamber in future if these parameters need to be controlled. Tests can be done for a wide range of temperature and relative humidity if required.

Holes are drilled into the metal base plate and two metal bars are mounted on the base plate to hold the specimen. Load cell is attached right below the displacement cell so that the load and displacement at the same point can be recorded. The displacement application bar is mounted on the load cell. Two holes are drilled into the specimen near two corners to mechanically fasten it to the supporting bars. These corners are selected as the fixed boundary as opposed to the midpoints of the two sides to seamlessly transition between two stable states. One hole is drilled at the center to fasten it to the displacement application bar. Displacement is applied at the center of the specimen to generate the actuation force required for snapthrough and snapback of the laminate during cyclic loading. WinTest software is utilized for providing the fatigue test input parameter values, data accumulation and retrieval. The system has to be tuned in displacement control with the same waveform parameters as the fatigue test before starting the test. Test conditions are as listed here:

1. Laminate Size: 3×3 inches
2. Ply Configuration: [0/90]
3. Waveform: Sinusoidal
4. Frequency, f = 1 HZ
5. U_{max} = 5.5 mm and U_{min} = -5.5 mm
6. Initial load = 8.29 N
7. Number of cycles, n = 3 million
8. Fastener Size: 5-40
9. Laminate is kept as flat as possible at the start of the test
10. Displacement cell is reset to zero
11. Load cell is kept as is and the magnitude of load is recorded to keep track of the residual stress
12. Displacement is applied at the center

2×2 and 3×3 inches samples were initially fabricated for testing. The 2×2 inches samples lost bistability after reaching moisture saturation at 65% RH. But the 3×3 inches samples maintained bistability despite experiencing reduction in curvature. This prompted the selection of the 3×3 inches specimen for fatigue test. It is an interesting phenomenon that needs to be investigated in future studies where a size dependent analysis of the moisture effect on the unsymmetric cross-ply laminates will be performed. Test conditions are laid out in such a way that a groundwork for the fatigue testing of bistable laminates is established by minimizing the number of parameters. That is why the simplest ply configuration, [0/90] required to achieve bistability and a sinusoidal waveform are chosen. A frequency of 1 Hz is selected to exclude any dynamic and heating effect on the specimen. ±5.5 mm peak to peak amplitude is chosen since it is well outside the maximum height that the specimen attains after moisture saturation but does not pass the factory limit of ±6.5 mm of the Bose Electroforce system set by the manufacturer. Test is done for 3 million cycles and the laminate is kept flat at the start of the test to ensure that one of the stable shapes is not stretched substantially more than the other. This adjustment requires a preload on the specimen before the test which is recorded so that this information can be utilized when necessary.

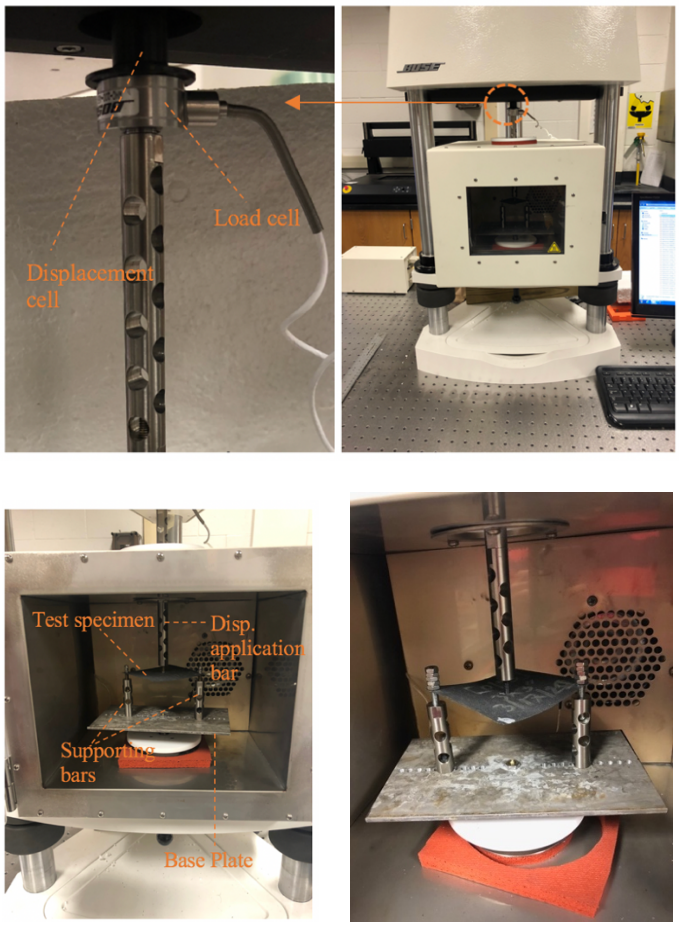

FIGURE 4: FATIGUE TEST FIXTURE

4. RESULTS AND DISCUSSION

4.1 Stiffness Degradation Analysis

Test is carried out in displacement control while the load response is measured. Load response with respect to displacement for a representative cycle is presented in Fig. 5 along with the two stable configurations achieved during the cycle. The sections in the plot corresponding to each stable configuration are marked by area enclosed with orange color. It can be seen that the load experiences a sudden drop at the unstable configuration. This region is marked with blue color and corresponds to the transition from one stable shape to the other. This is consistent with the findings from previous studies [48,49] where bistable laminates loaded in displacement control also tracked load drop at the unstable configuration. The cycle starts from first stable configuration, experiences load drop at the unstable configuration, then reaches the second stable state during the first half of the cycle and completes the snapthrough process. In the second half of the cycle, it starts from second stable configuration, then unstable configuration, and finally comes back to the first stable configuration completing the snapback process. Thus, the specimen snaps between two stable states during each cycle in the time period of 1 second. This is also evident in the corresponding load vs. displacement plot for the cycle presented.

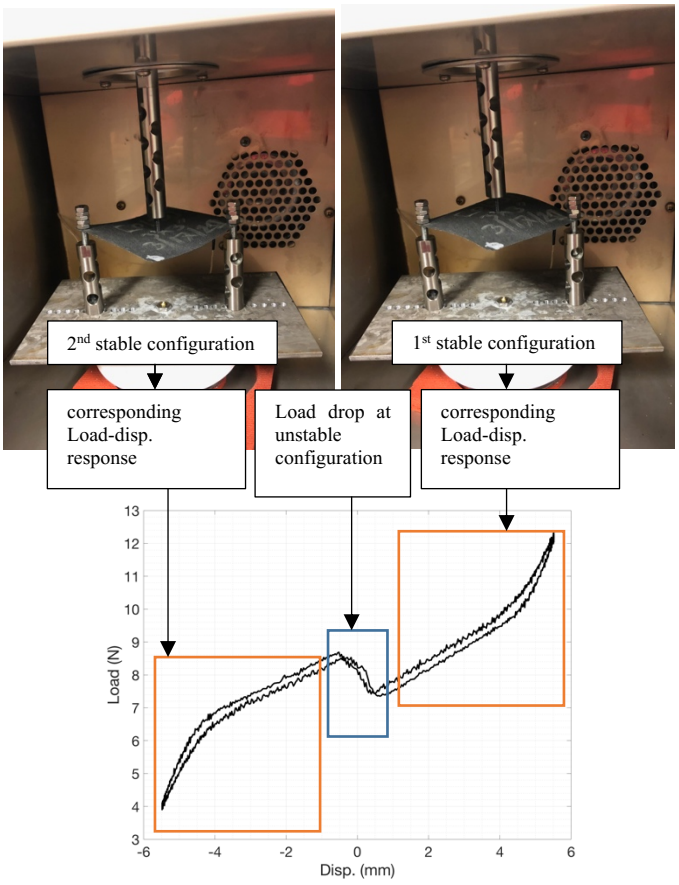

FIGURE 5: TWO STABLE CONFIGUARATIONS AND THE CORRESPONDING LOAD VS. DISP. PLOT ACQUIRED DURING ONE CYCLE

A 3"×3" specimen is tested with the aforementioned test conditions up to 3 million cycles. Time, displacement, and load data are retrieved for the test. The test was not run for 3 million cycles all at once, rather it was stopped and started again after every few thousand cycles. This was done to accumulate and analyze the data in a regular interval and investigate any change in bistability and stiffness. Typically, this was done every 500000 cycles. After the completion of 3 million cycles, disp. vs. load plot for cycle no. 10, 500000, 1 million, 2 million, and 3 million are plotted together as shown in Fig. 6 (A). Load-displacement plot forms a loop as expected from a cyclic test. Results unveil that the laminate maintains bistability after 3 million cycles as the shape of the curve remains unchanged.

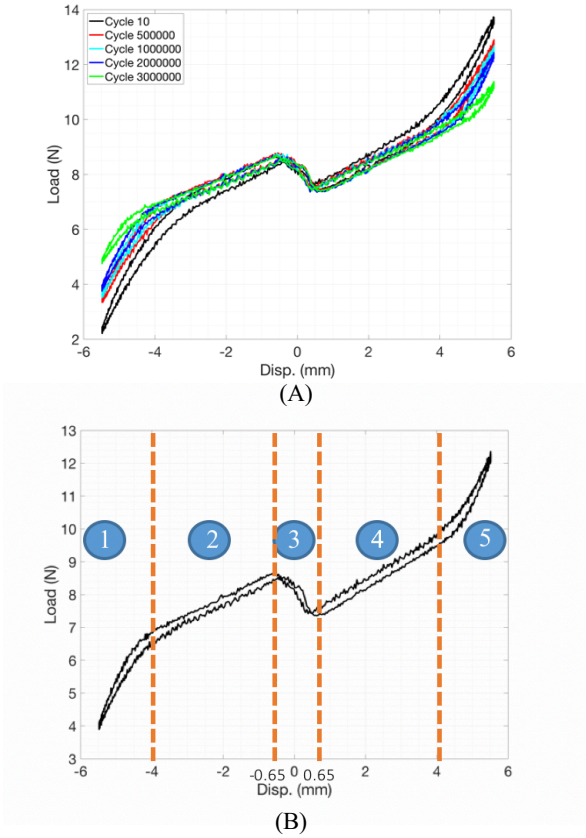

FIGURE 6: (A) LOAD-DISPLACEMENT PLOT FOR DIFFERENT NUMBER OF CYCLES (B) LOAD-DISPLACEMENT PLOT WITH 5 STIFFNESS REGIONS

Stiffness degradation is demonstrated by the load-displacement plot over the fatigue loading of 3 million cycles in Figure 6 (A). But degradation does not happen uniformly over the entire cycle. To quantify the stiffness degradation with good accuracy, one cycle is divided into five regions as illustrated in Figure 6 (B). The regions are outlined as region 1 from -5.5 mm to -4 mm, region 2 from -4 mm to -0.65 mm, region 3 from -0.65

mm to 0.65 mm, region 4 from 0.65 mm to 4 mm, and region 5 from 4 mm to 5.5 mm. Stiffness is defined as the slope of the curve in each region and acquired from a linear fit of the test data. Since all the regions are interpreted with linear models, the coefficient of determination R^2 can be considered as an adequate parameter to define the accuracy of the linear fit. The least R^2 value for the 1 Hz test is higher than 0.9. This means that more than 90% of the variability in the data is explained by the linear model which is characteristic of model with good accuracy. Stiffness determined this way is plotted over 3 million cycles in Figure 7 for a representative specimen. Taking this piecewise approach, stiffness degradation has been captured in all five regions.

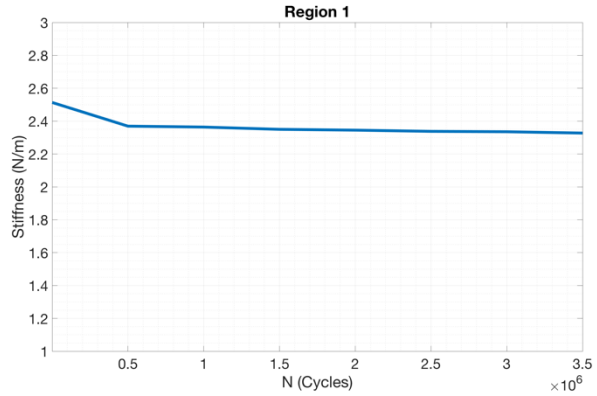

(A)

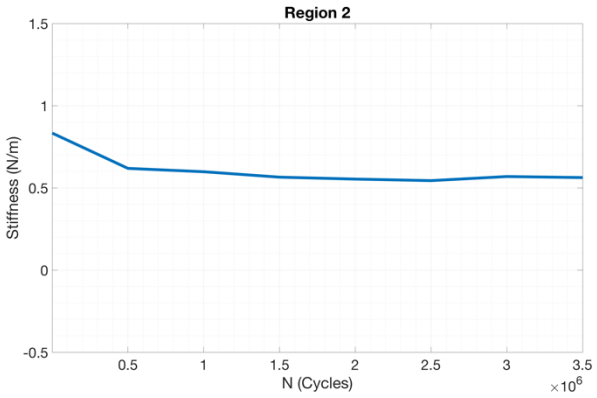

(B)

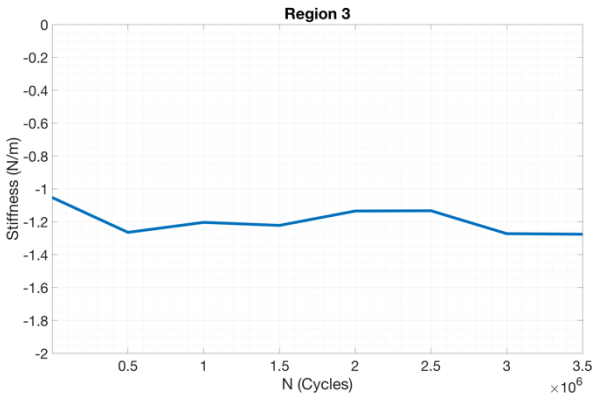

(C)

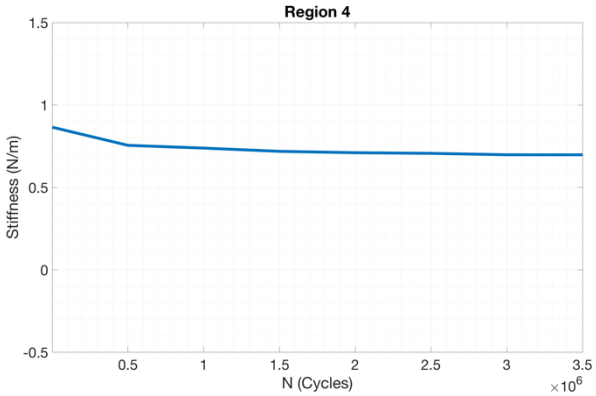

(D)

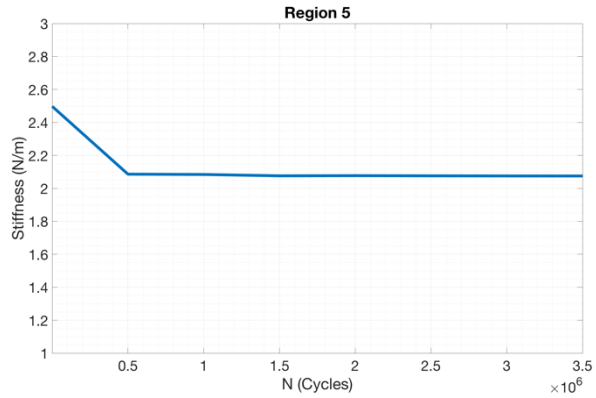

(E)

FIGURE 7: STIFFNESS DEGRADATION IN ALL REGIONS

4.2 Fatigue Damage Model

4.2.1 Shiri Model with Updated Approach

Stiffness degradation and accumulation of fatigue damage in composite materials have been investigated and appropriate mathematical models have been presented utilizing the test data in a series of studies [44,50–54]. Damage progression is explained in the same three stages as stiffness degradation. In this study the predictive model presented by Shiri is chosen due to its accuracy of fitting for different materials, improved adaptability for a wide spectrum of loading conditions, and a minimum number of required model parameters [44]. In this model, a damage index is defined with trigonometric terms to predict the damage progress in all three stages. The fatigue damage model can be outlined with the following expression

$$D\,(n) = \frac{E_0 - E(n)}{E_0 - E_f} = \frac{sin\,(qx)cos(q-p)}{sin\,(q)cos(qx-p)} \qquad (1)$$

Where, $D\ (n)$ is the fatigue damage index which is expressed as the ratio of the residual modulus at the nth cycle and the final failure cycle. E_0, $E(n)$, and E_f are elastic modulus of the initial cycle, nth cycle, and final failure cycle respectively.

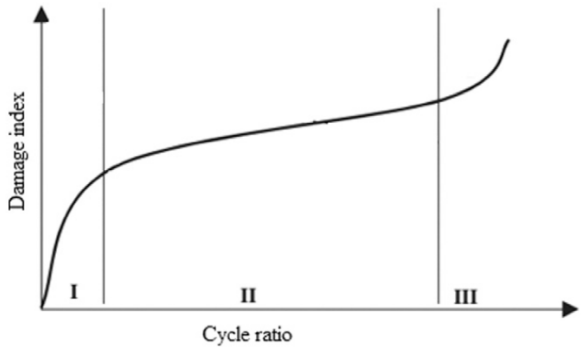

FIGURE 8: FATIGUE DAMAGE EVOLUTION IN COMPOSITES [44]

In the present study, stiffness is utilized in place of elastic modulus to determine damage from test data. This stiffness is defined as the slope of the load displacement plot in each region. The trigonometric expression is an empirical formulation to capture the damage evolution with respect to number of cycles. Damage defined with elastic modulus in Shiri's study had good agreement with this model. Trend of damage from the present study where damage is defined with stiffness, had a similar curvature in the damage vs cycle plot. So, utilizing the same trigonometric formulation to capture damage in our study is considered a reasonable adoptation. Current number of cycles is denoted with n while N is the Fatigue failure cycle. The normalized cycle ratio is defined as $x = n/N$. Material dependent parameters p, and q can be determined by fitting the model to test data. These parameters are determined for each stiffness region by performing regression analysis in a piecewise approach. Damage index from test data, D is defined with the following expression

$$D = 1 - \frac{Stiffness\ at\ nth\ cycle}{Stiffness\ at\ initial\ cycle} \qquad (2)$$

Regression analysis is performed according to the principle of the minimization of the residual sum of squares. In this method, the difference between the measured damage index and the predicted damage index from the model for all the observations are determined. The sum of the squares of these differences is the residual sum of squares or RSS. Parameters p, q are determined for the minimum value of the RSS. Damage progression over 3 million cycles from the test data and the damage prediction from Shiri model with the determined model parameters are plotted together for regions 1, 2, 4, and 5 in Figure 9 (A) –(D). The unstable region is not considered for this analysis. Model parameter values determined from fitting the test data are presented with each respective region. These parameters are tabulated in Table 2 and it can be seen that the p, q values are fairly consistent among the 4 regions. This is not the case for the

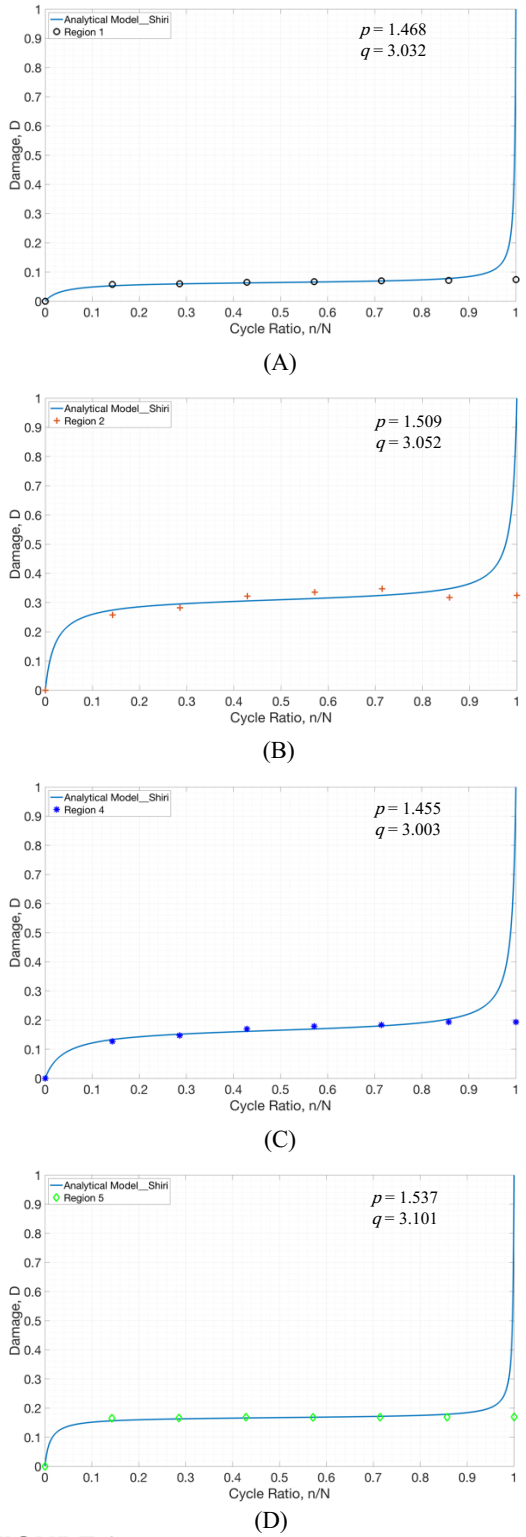

FIGURE 9: FATIGUE DAMAGE EVOLUTION IN COMPOSITES DAMAGE PROGRESSION FROM 1 HZ TEST DATA AND SHIRI MODEL FIT FOR REGIONS 1, 2, 4, AND 5

Wu model that will be discussed in the following section. As failure has not occurred during the fatigue test, 3 million cycles is assigned as the value of N. This explains the deviation of the prediction from the observation at 3 million cycles. Model parameter values are in close range with the values presented in previous studies. Overall, this piecewise analysis with the Shiri model has captured the damage progression for 1 Hz test with high accuracy and have the potential to be applied with different laminate sizes and ply configurations of bistable composites.

Region	Shiri Model Material Parameters		Wu Model Material Parameters	
	p	q	A	B
Region 1	1.468	3.032	0.089	0.057
Region 2	1.509	3.052	0.219	0.076
Region 4	1.455	3.003	0.058	0.007
Region 5	1.537	3.101	0.101	0.055

TABLE 2: MATERIAL PARAMETERS DETERMINED FROM SHIRI AND WU MODEL FOR ALL 4 STIFFNESS REGIONS

4.2.1 Wu Model with Updated Approach

Similar analysis is performed with another model proposed by Wu [51] which is expressed as

$$D\,(n) = \frac{E_0 - E(n)}{E_0 - E_f} = 1 - \left(1 - \left(\frac{n}{N}\right)^B\right)^A \qquad (3)$$

Where all the parameters are defined like Shiri model. This model was fitted with the test data to determine the model parameter values for minimum RSS and compare the prediction following the same procedure. Figure 10 (A)-(D) exhibits that Wu model also provides moderately good prediction of the fatigue damage. But it tends to overpredict the damage at initial 10 cycles for all the regions. The model captures both stages of the fatigue test represented by the test data with reasonable accuracy but the prediction is not as good as the Shiri model especially in region 2 and 5. Model parameters A and B differ by one to several orders of magnitude for different regions compared to previous studies. So, the piecewise approach is also capable of predicting fatigue damage with the Wu model with some limitations. Evaluation of the two models determines the Shiri model to have the higher potential for fatigue analysis. Tests with 1 Hz frequency can be considered to be at steady state and responses in this range can be predicted with these models in the proposed approach. Test data have been reproduced and representative data from one specimen is presented in this analysis.

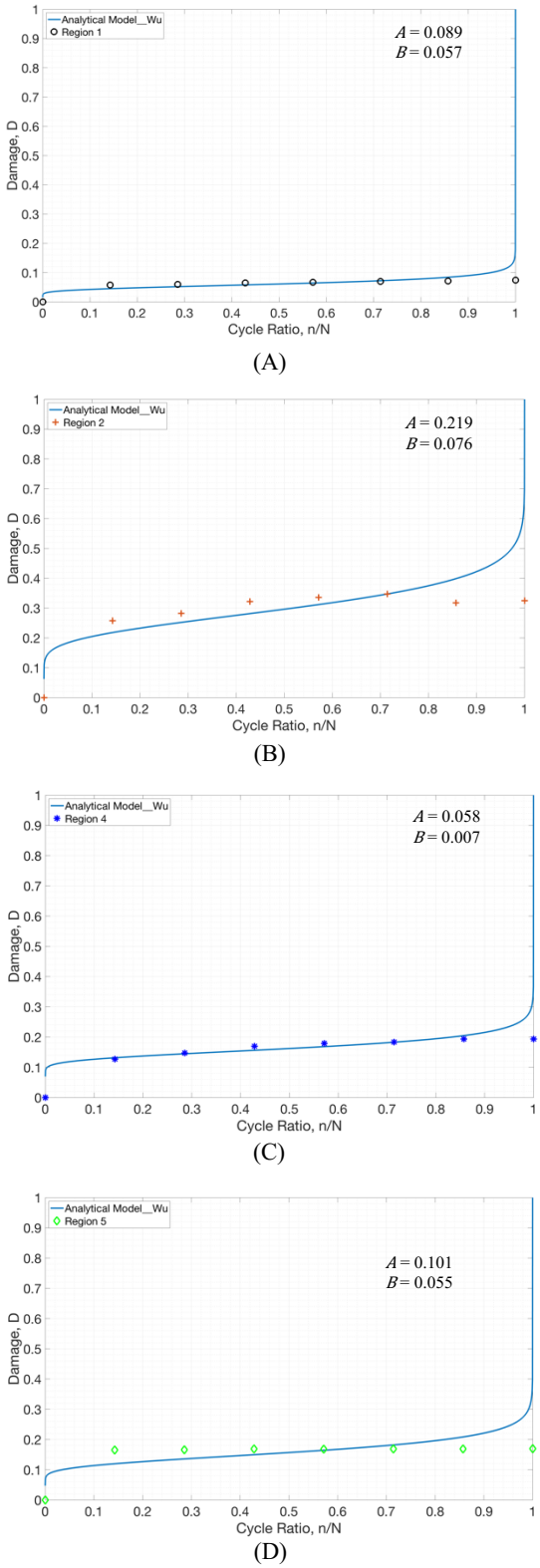

FIGURE 10: DAMAGE PROGRESSION FOR 1 HZ TEST FROM TEST DATA AND WU MODEL FIT FOR REGIONS 1, 2, 4, AND 5

4. CONCLUSION

Response of bistable laminates to long term fatigue is an important phenomenon which has been studied in this analysis. Tests are performed at 1 Hz frequency up to 3 million cycles at specified loading condition. Stiffness degradation of the specimen is captured in a piecewise manner and a damage index is introduced in terms of stiffness degradation to represent damage progression over the duration of the test. Two analytical models, Shiri and Wu model have been evaluated for damage prediction and both models demonstrated good accuracy when compared with test data while the Shiri model was determined to provide better prediction of fatigue damage progression. This investigation lays the groundwork for fatigue tests of multistable laminates at different frequencies, and loading conditions.

Acknowledgement

The authors acknowledge the support from National Science Foundation (CMMI-1760943). The authors also acknowledge Vishrut Deshpande for his valuable feedback and constructive suggestions during the development of test fixture and subsequent analysis.

REFERENCES

[1] Schultz, M. R., 2008. "A concept for airfoil-like active bistable twisting Structures". *Journal of Intelligent Material Systems and Structures,* **19**, pp. 157–69.

[2] Hyer, M. W., 1981. "Some Observations on the Cured Shape of Thin Unsymmetric Laminates". *Journal of Composite Materials,* **15**.

[3] Hufenbach, W. and Gude, M., 2002. "Analysis and optimisation of multistable composites under residual stresses". *Composite Structures,* **55**.

[4] Gandhi, Y., Pirondi, A., and Collini, L., 2018. "Analysis of bistable composite laminate with embedded SMA actuators". *Procedia Structural Integrity,* **12**.

[5] Thill, C., Etches, J., Bond, I., Potter, K., and Weaver, P., 2008. "Morphing skins". *The Aeronautical Journal,* **112**.

[6] Lachenal, X., Daynes, S., and Weaver, P. M., 2013. "Review of morphing concepts and materials for wind turbine blade applications". *Wind Energy,* **16**.

[7] Daynes, S., and Weaver, P. M., 2013. "Review of shape-morphing automobile structures: concepts and outlook". *Proceedings of the Institution of Mechanical Engineers, Part D: Journal of Automobile Engineering,* **227**.

[8] Giddings, P. F., Bowen, C. R., Salo, A. I. T,, Kim, H. A., and Ive, A., 2010. "Bistable composite laminates: Effects of laminate composition on cured shape and response to thermal load". *Composite Structures,* **92**.

[9] Schultz, M. R., and Hyer, M. W., 2003. "Snap-Through of Unsymmetric Cross-Ply Laminates Using Piezoceramic Actuators". *Journal of Intelligent Material Systems and Structures,* **14**.

[10] Schultz, M. R., Hyer, M. W., Brett, Williams, R., Keats, Wilkie, W., and Inman, D. J., 2006. "Snap-through of unsymmetric laminates using piezocomposite actuators". *Composites Science and Technology,* **66**.

[11] Gude, M., and Hufenbach, W., 2006. "Design of novel morphing structures based on bistable composites with piezoceramic actuators". *Mechanics of Composite Materials,* **42**.

[12] Giddings, P., Bowen, C. R., Butler, R., and Kim, H. A., 2008. "Characterisation of actuation properties of piezoelectric bi-stable carbon-fibre laminates". *Composites Part A: Applied Science and Manufacturing,* **39**.

[13] Bowen, C. R., Butler, R., Jervis, R., Kim, H. A., and Salo, A. I. T., 2007. "Morphing and Shape Control using Unsymmetrical Composites". *Journal of Intelligent Material Systems and Structures,* **18**.

[14] Harne, R. L., and Wang, K. W., 2013. "A review of the recent research on vibration energy harvesting via bistable systems". *Smart Materials and Structures,* **22**.

[15] Degrieck, and J., and van, Paepegem, W., 2001. "Fatigue damage modeling of fibre-reinforced composite materials: Review". *Applied Mechanics Reviews,* **54**.

[16] Hashin, Z., and Rotem, A., 1973. "A Fatigue Failure Criterion for Fiber Reinforced Materials". *Journal of Composite Materials,* **7**.

[17] Hwang, W., and Han, K. S., 1986. "Fatigue of Composites—Fatigue Modulus Concept and Life Prediction", *Journal of Composite Materials,* **20**.

[18] Kam, T. Y., Chu, K. H., and Tsai, S. Y., 1998. "Fatigue reliability evaluation for composite laminates via a direct numerical integration technique". *International Journal of Solids and Structures,* **35**.

[19] Kam, T. Y., Tsai, S. Y., and Chu, K. H., 1997. "Fatigue reliability analysis of composite laminates under spectrum stress". *International Journal of Solids and Structures,* **34**.

[20] Fatemi A and Yang L 1998 Cumulative fatigue damage and life prediction theories: a survey of the state of the art for homogeneous materials *International Journal of Fatigue* **20**.

[21] Sidoroff, F., and Subagio, B., 1987. "Fatigue damage modeling of composite materials from bending tests". *Int Conf on Composite Materials (ICCM-VI) & Second European Conf on Composite Materials (ECCM-II),* (London).

[22] van, Paepegem, W., and Degrieck, J., 2000. "Numerical modeling of fatigue degradation of fibre-reinforced composite materials". *5th Int Conf on Computational Structures Technology,* (Leuven).

[23] van, Paepegem, W., and Degrieck, J., 2001. "Experimental setup for and numerical modeling of bending fatigue experiments on plain woven glass/epoxy composites". *Compos. Struct*

[24] Chou, P., and Croman, R., "Degradation and Sudden-Death Models of Fatigue of Graphite/Epoxy

Composites". *Fifth Conference on Composite Materials: Testing and Design,* (100 Barr Harbor Drive, PO Box C700, West Conshohocken, PA 19428-2959: ASTM International).

[25] Halpin, J., Jerina, K., and Johnson, T., "Characterization of Composites for the Purpose of Reliability Evaluation". *Analysis of the Test Methods for High Modulus Fibers and Composites,* (100 Barr Harbor Drive, PO Box C700, West Conshohocken, PA 19428-2959: ASTM International).

[26] Yang, J. N., 1978. "Fatigue and Residual Strength Degradation for Graphite/Epoxy Composites Under Tension-Compression Cyclic Loadings". *Journal of Composite Materials,* **12**.

[27] Kedward, K., and Beaumont, P., 1992. "The treatment of fatigue and damage accumulation in composite design". *International Journal of Fatigue,* **14**.

[28] Yang, J. and Jones, D., "Load Sequence Effects on the Fatigue of Unnotched Composite Materials". *Fatigue of Fibrous Composite Materials,* (100 Barr Harbor Drive, PO Box C700, West Conshohocken, PA 19428-2959: ASTM International).

[29] Owen, M.J., and Bishop, P.T., 1974. "Prediction of static and fatigue damage and crack propagation in composite materials". *Advisory Group for Aerospace Research and Development ~AGARD.*

[30] Biner, S. B. and Yuhas, V. C., 1989. "Growth of Short Fatigue Cracks at Notches in Woven Fiber Glass Reinforced Polymeric Composites". *Journal of Engineering Materials and Technology,* **111**.

[31] Bergmann, H. W., and Prinz, R., 1989. "Fatigue life estimation of graphite/epoxy laminates under consideration of delamination growth". *International Journal for Numerical Methods in Engineering,* **27**.

[32] Prinz, R., 1990. "Damage Rates for Interlaminar Failure of Fatigued CFRP Laminates". *Developments in the Science and Technology of Composite Materials,* (Dordrecht: Springer Netherlands).

[33] Dahlen, C., and Springer, G. S., 1994. "Delamination Growth in Composites under Cyclic Loads". *Journal of Composite Materials* **28**.

[34] Panduranga, R., and Shivakumar, K., 2017. "Mode-II total fatigue life model for unidirectional IM7/8552 carbon/epoxy composite laminate", *International Journal of Fatigue,* **94**.

[35] Pipes, R. B., and Pagano, N. J., 1994. "Interlaminar Stresses in Composite Laminates Under Uniform Axial Extension".

[36] O'Brien, T., "Characterization of Delamination Onset and Growth in a Composite Laminate", *Damage in Composite Materials: Basic Mechanisms, Accumulation, Tolerance, and Characterization,* (100 Barr Harbor Drive, PO Box C700, West Conshohocken, PA 19428-2959: ASTM International).

[37] Pagano, N. J., 1989. "Interlaminar Response of Composite Materials". *Composite Materials Series,* **5**.

[38] Salpekar, S. A., O'Brien, T. K. and Shivakumar, K. N., 1996. "Analysis of Local Delaminations Caused by Angle Ply Matrix Cracks". *Journal of Composite Materials,* **30**.

[39] Saunders, D. S., Galea, S. C., and Deirmendjian, G. K., 1993. "The development of fatigue damage around fastener holes in thick graphite/epoxy composite laminates". *Composites,* **24**.

[40] Peng, T., Liu, Y., Saxena, A., and Goebel, K., 2015. "In-situ fatigue life prognosis for composite laminates based on stiffness degradation". *Composite Structure,s* **132**, pp. 155–65.

[41] Varvani-Farahani, A., and Shirazi, A., 2007. "A Fatigue Damage Model for (0/90) FRP Composites based on Stiffness Degradation of 0° and 90° Composite Plies". *Journal of Reinforced Plastics and Composites,* **26**.

[42] Reifsnider, K. L., 1991. "Damage and Damage Mechanics". *Composite Materials Series,* **4**, pp. 11-77.

[43] Potter, K., 2006. "Measurements of the snap-through behaviour and snap-through fatigue performance *of bistable unsymmetric composite structures". 3rd international conference on composite testing and model identification, Porto, Portugal,* pp. 10-12.

[44] Shiri, S., Yazdani, M., and Pourgol-Mohammad, M., 2015. "A fatigue damage accumulation model based on stiffness degradation of composite materials". *Materials and Design,* **88**, pp. 1290–5.

[45] Lele, A. G., 2018. *TigerPrints An Investigative Study of the Snapthrough, Snapback and the Stiffness Properties of a Kirigami Unit Cell.*

[46] Biegler, K., *OWNERS MANUAL,3200 SERIES III.*

[47] Anon *WinTest ® 7 Software Reference Manual.*

[48] Mattioni, F., Weaver, P. M., Potter, K. D., and Friswell, M. I., 2008. "Analysis of thermally induced multistable composites". *International Journal of Solids and Structures,* **45**.

[49] Tawfik, S., Tan, X., Ozbay, S., and Armanios, E., 2007. "Anticlastic Stability Modeling for Cross-ply Composites". *Journal of Composite Materials,* **41**.

[50] Whitworth, H. A., 1997. "A stiffness degradation model for composite laminates under fatigue loading". *Composite Structures,* **40**.

[51] Wu, F., and Yao, W., 2010. "A fatigue damage model of composite materials". *International Journal of Fatigue,* **32**.

[52] Tate, J. S., and Kelkar A. D., 2008. "Stiffness degradation model for biaxial braided composites under fatigue loading". *Composites Part B: Engineering,* **39**.

[53] Shirazi, A., and Varvani-Farahani, A., 2010. "A Stiffness Degradation Based Fatigue Damage Model for FRP Composites of (0/θ) Laminate Systems". *Applied Composite Materials,* **17**.

[54] Yang, J. N., Jones, D. L., Yang, S. H., and Meskini, A., 1990. "A Stiffness Degradation Model for Graphite/Epoxy Laminates". *Journal of Composite Materials,* **24**.